Submitted to *Journal of Geophysical Research* (Space Physics): September 21, 2000.

Heating of the Low-Latitude Solar Wind by Dissipation of Turbulent Magnetic Fluctuations

Charles W. Smith, William H. Matthaeus, Gary P. Zank and Norman F. Ness

Bartol Research Institute, University of Delaware, Newark

Sean Oughton

Department of Mathematics, University College London

John D. Richardson

Massachusetts Institute of Technology, Cambridge

Abstract. We test a theory presented previously to account for the turbulent transport of magnetic fluctuation energy in the solar wind and the related dissipation and heating of the ambient ion population. This theory accounts for the injection of magnetic energy through the damping of large-scale flow gradients such as wind shear and compression, and incorporates the injection of magnetic energy due to wave excitation by interstellar pickup ions. The theory assumes quasi-2D spectral transport of the fluctuation energy and subsequent dissipation that heats the thermal protons. We compare the predictions of this theory with Voyager 2 and Pioneer 11 observations of magnetic fluctuation energy, magnetic correlation lengths, and ambient proton temperatures. Near-Earth Omnitape observations are used to adjust for solar variability and the possibility that high-latitude effects could mask possible radial dependences is considered. We find abundant evidence for in situ heating of the protons, which we quantify, and show that the observed magnetic energy is consistent with the ion temperatures.

1. Introduction

For a long time, two contrasting paradigms have attempted to describe the nature and evolution of the low-frequency fluctuations of the interplanetary magnetic field (IMF) and associated thermal proton moments (density, velocity, and temperature) in the solar wind. In the first, fluctuations in the wind and IMF are presumed to be waves, most likely Aflvén waves, that are remnant signatures propagating out of the solar corona [*Coleman*, 1966; *Belcher and Davis*, 1979; *Barnes*, 1979]. In the second, the fluctuations arise in situ as a result of large-scale interplanetary sources such as wind shear and evolve nonlinearly in a manner analogous to traditional hydrodynamic turbulence [*Coleman*, 1968]. Single-point measurements are largely incapable of resolving the issue as the two viewpoints often predict, or are consistent with, similar single-point measurements (possible high correlation between the magnetic and velocity field fluctuations, density fluctuations that are small and correlated with field fluctuations, magnetic and velocity fluctuations that are transverse to the mean magnetic field, minimum variance directions that are aligned with the mean field, etc.). The most descriminating test of the two viewpoints requires that the evolution of the system be examined and compared with predictions for the two paradigms.

Low-frequency Alfvén waves are generally thought

to evolve according to leading-order WKB theory [*Hollweg*, 1973, 1974, 1990] wherein the wave evolves according to a noninteracting dynamic that preserves the identity of each individual wave. Any dissipation mechanism which is active within the plasma is expected to leave voids in the spectrum as replenishment cannot occur without some postulated additional source. For this reason, there is a natural limit to the heating rate [*Schwartz et al.*, 1981]. The turbulence viewpoint is that the fluctuations (some of which may be wave-like) represent inherently nonlinear modes of the system. Such fluctuations are constantly interacting and energy is transferred between the various spatial scales represented in the spectrum [*Kraichnan and Montgomery*, 1980; *Matthaeus et al.*, 1995]. In the latter viewpoint, the large-scale sources of the energy act to replenish the smaller scales and resupply the dissipation mechanism. The heating rate is at least partially dictated by the spectral transfer rate from the large "energy containing" scales to the small scales.

We can demonstrate these ideas by writing a simplified, general expression for the transport of turbulent energy:

$$\frac{\partial Z^2}{\partial t} + V_{SW}\frac{\partial Z^2}{\partial r} + \frac{A}{r}Z^2 = D + S \qquad (1)$$

where V_{SW} is the solar wind speed and r is the heliocentric distance. $Z^2 = \langle v^2 + b^2 \rangle$ is the ensemble-averaged fluctuation energy density expressed in Elsässer variables with v the solar wind velocity fluctuation. The magnetic field B is expressed in Alfvén units

$$b = \delta B / \sqrt{4\pi\rho}, \qquad (2)$$

where δB is the magnetic field fluctuation relative to the local mean field $\langle B \rangle = B_0$ and ρ is the mass density. D represents the general driving terms while S collects the sink (or dissipation) terms. The prediction for stationary WKB theory can be obtained by setting $\partial Z^2/\partial t = 0$, $A = 1$, $D = 0$ and $S = 0$ to get $Z^2_{WKB} \sim r^{-1}$. Taking into account that $\rho \sim r^{-2}$, we obtain the WKB prediction for the radial evolution of magnetic energy $(\delta B)^2 \sim r^{-3}$. The source terms are then capable of elevating the magnetic energy above the WKB prediction while the sink terms reduce the magnetic fluctuations in favor of heating the background particles. Correct determination of D indirectly regulates the dissipation processes by controlling the level of energy available for dissipation by the sink terms.

A number of studies address the purported turbulent evolution of solar wind fluctuations by examining transport equations for inertial range fluctuations [*Zhou and Matthaeus*, 1990; *Verma and Roberts*, 1993; *Tu and Marsch*, 1995]. *Zank et al.* [1996] offer an early test of the turbulence paradigm for the energy-containing range by examining the radial variation of IMF fluctuation energy using Voyager 1 and 2 and Pioneer 11 observations. The observations are seen to possess more energy than the simple WKB prediction, but significantly less energy than a modified form of WKB with enhanced driving by pickup ions. In the latter prediction, the pickup ions excite additional wave energy that is unable to dissipate significantly in the WKB model so that the prediction accumulates too much magnetic energy in the outer heliosphere. Observations of IMF fluctuation energy beyond about 10 AU are too large to be explained by the turbulence model if wind shear alone drives the turbulence, but are consistent with the turbulence model if both wind shear and pickup ions drive the turbulence. If dissipation is as critical as the above suggests, then the thermal protons must exhibit a signature of this in situ heating.

Richardson et al. [1995] performed an analysis of thermal proton distributions observed by Voyager 2 from launch until late 1994 when the spacecraft was at 42 AU. A fit of proton temperatures T produced the result that $T = 3.77 \times 10^4\ r^{-0.49 \pm 0.01}$ where r is the heliocentric distance measured in AU. Arguably, this fit begins to degrade beyond ~25 AU where the observed proton temperatures are falling less rapidly than the fit function, but this is not unambiguously clear until the data is extended to 1998 as we will show in this paper. Richardson et al. observe that the apparent disagreement may be the result of energy injected by the pickup of interstellar neutrals, but also add that other explanations including latitudinal and solar cycle effects are possible. In a related paper, *Richardson et al.* [1996] examine the thermal anisotropy of the ambient proton population observed by the Voyager 2 spacecraft and provide additional evidence for heating, possibly via the pickup of interstellar neutrals. While the radial temperature dependence reported by *Richardson et al.* [1995], and given further examination in this paper, neglects anisotropy, the anisotropy is not large enough to significantly complicate this analysis.

Gazis and Lazarus [1982] fit a shorter interval of this same Voyager dataset from 1 to 10 AU to obtain $T \propto r^{-0.7}$. Both results are easily distinguished

from the $T \sim r^{-4/3}$ prediction of adiabatic expansion and provide strong indications that heating of the solar wind protons occurs within 20 AU. *Gazis* [1994] argues that latitudinal effects may be the dominant consideration in evaluating the radial dependence of Voyager proton temperatures, and so we will address this issue in section 3. Observations by the Helios spacecraft [*Freeman*, 1988] are indicative of interplanetary heating inside 1 AU, particularly for intervals with solar wind speed $V_{SW} > 500\,\mathrm{km\,s^{-1}}$.

Matthaeus et al. [1999] provide a preliminary examination of solar wind heating and a comparison with turbulence predictions [*Marsch and Tu*, 1989; *Zhou and Matthaeus*, 1990; *Matthaeus et al.*, 1996]. Using only Voyager 2 observations, they demonstrate that the radial evolution of the correlation length for IMF fluctuations is accurately predicted by the theory. In addition, and more importantly, they show that the radial variation of the proton temperature agrees with predictions derived from a theory of two-dimensional turbulence driven by wind shear and pickup ions. However, neither *Zank et al.* [1996] nor *Matthaeus et al.* [1999] consider variations due to solar cycle and spacecraft latitude. In this paper we examine both of these issues and provide a more descriminating demonstration of the validity of this theory.

As with *Zank et al.* [1996] and *Matthaeus et al.* [1999], we consider two energy sources for driving turbulence, leading to enhanced in situ heating of the interplanetary ions: wind shear and newborn interstellar pickup ions. We will argue that the former is most active for $r < 20$ AU while the latter is active only outside the ionization cavity ($r > 8$ AU). As a source for thermal proton heating, wind shear generates low-frequency magnetic fluctuations predominantly in the energy-containing range at scales much larger than either the proton gyroradius or the ion inertial length. This energy must be transported to smaller spatial scales where various kinetic dissipation processes can convert the organized plasma fluctuations into heat. In section 2 we will describe a theory for the turbulent transport of magnetic energy that does exactly this without consideration for the details of the actual dissipation mechanism. It is an assumption of the turbulence model that the energy dissipation rate is governed by the rate of energy transfer through the inertial range, and not the specific mechanism of magnetic energy dissipation.

While the pickup process can also excite high-frequency waves [*Gray et al.*, 1996] that may directly heat the background ions, it is commonly held that most of the energy deposition is in the form of Alfvén waves at larger spatial scales [*Lee and Ip*, 1987]. The dynamics of the dominant Alfvén wave energy deposition involves the scattering of newborn ions out of their initial ring-beam distribution with concommittent generation of MHD waves [see *Zank*, 1999 for a review]. If one assumes that the scattering rapidly leads to a bispherical shell [*Johnstone et al.*, 1991; *Williams et al.*, 1995] then one can estimate that this process liberates $\sim 10\%$ of the pickup energy for the excitation of magnetic waves. Regardless of the details, the newly injected wave energy participates in the same turbulent transport of energy to the dissipation scales.

It should be noted that the above estimate for the energy in the pickup ion-excited waves is very crude and subject to several important assumptions. As we discuss below, the energy estimate derived from a quasilinear theory bispherical calculation should be regarded as an upper limit only. Implicit in the assumption that the asymptotic ion distribution is a bispherical distribution is the assumption that the pickup ions lose a *maximum* amount of energy to waves and that the ions experience no energization beyond the shell distribution of radius V_{SW}.

In the section that follows we outline a theory for the turbulent heating of the solar wind thermal ions through the cascade of energy from large-scale sources to the dissipation scales. The two energy sources that will be considered are wind shear and waves due to newborn pickup ions. In section 3 we analyze Voyager 2 and Pioneer 11 data in a test of the theory. We close by summarizing our results and provide two appendices that attempt to describe uncertainties in this (and potentially any) analysis of the correlation length of IMF fluctuations as well as revealing some of the uncertainty in our choices of theoretical parameters.

2. Theory

Three principle sources exist for turbulence in the outer heliosphere. The first is shear associated with the interaction of fast and slow speed streams [*Coleman*, 1968] and the second is compressional effects associated with both stream-stream interactions and shock waves. The third source, which occurs beyond the ionization cavity, is turbulence generated by wave-particle interactions associated with the ionization of interstellar hydrogen. Both the shear and compres-

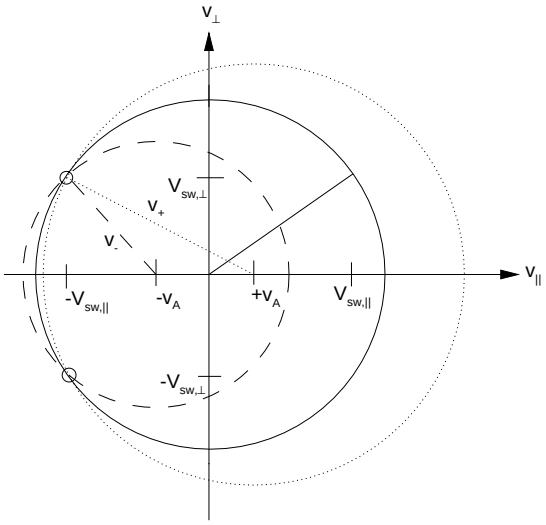

Figure 1. The bispherical distribution is composed of the dotted circle for $v_{||} < -V_{SW,||}$ and the dashed circle for $v_{||} > -V_{SW,||}$ where $||$ / $\perp$ indicates parallel/perpendicular to the IMF and v is the particle velocity.

sional source terms can be scaled approximately as [*Zank et al.*, 1996]

$$\dot{E}_{shear(comp)} = C_{shear(comp)} \frac{V_{SW}}{r} Z^2, \qquad (3)$$

where $C_{shear(comp)}$ are prescribed constants.

The ionization of interstellar neutral H introduces an unstable ring-beam distribution of pickup ions into the solar wind. The pickup ions are assumed to scatter in pitch-angle by excited and ambient low-frequency waves while preserving their energy in the wave frame (see Figure 1). If the pickup ion generated (unstable) parallel-propagating modes dominate the fluctuation spectrum, then the pickup ions scatter onto partial shells centered on $\pm V_A$ (dotted and dashed circles in Figure 1) where V_A is the Alfvén speed, and asymptotically onto a "bispherical" shell distribution. This is to be contrasted with elastic scattering in the solar wind frame, which would yield a spherical distribution (solid curve). The difference in kinetic energy between the spherical and bispherical distributions is given to the waves and their free energy is $\sim V_A/V_{SW}$ of the initial pickup ion number density [*Williams and Zank*, 1994]. The source term for pickup ion generated turbulence is [*Williams and Zank*, 1994]

$$\begin{aligned} \dot{E}_{PI} &= \frac{\mathrm{d}n_{PI}}{\mathrm{d}t} \frac{V_A V_{SW}}{n_{SW}} \\ &= \frac{V_{SW} V_A n_H^{\infty}}{n_{SW}^{o} \tau_{ion}^{o}} \exp\left[-\lambda_{PI}\theta / r \sin\theta\right], \end{aligned} \qquad (4)$$

where $n_{PI,SW}$ denote pickup ion and solar wind number densities, respectively, and the time derivative refers to a creation rate rather than an advective derivative. We take n_{SW}^{0}, the thermal proton density at 1 AU, to be $5\,\mathrm{cm}^{-3}$. We assume V_A to be $50\,\mathrm{km\,s}^{-1}$ at all heliocentric distances and $V_{SW} = 400\,\mathrm{km\,s}^{-1}$. We express the pickup ion creation rate in terms of the cold gas interstellar neutral distribution approximation and n_H^{∞} should be interpreted as the neutral number density at the termination shock. This approximation is reasonable provided n_H^{∞} is chosen properly and we take $n_H^{\infty} = 0.1\,\mathrm{cm}^{-3}$. Finally, τ_{ion}^{0} is the neutral ionization time at 1 AU which we take to be 10^6 s, λ_{PI} is the ionization cavity length scale which we take to be 8 AU, and θ the angle between the observation point and the upstream direction which we take to be 0°.

The parameters used in equation 4 should also be viewed cautiously. Equation 4 assumes a cold neutral H distribution [*Vasyliunus and Siscoe*, 1976], which is certainly an inaccurate representation of interstellar neutral H in the heliosphere [see *Zank*, 1999 for an extensive review of the hot and cold neutral H models]. The scale length of the ionization cavity λ_{PI} can vary with solar cycle, as can the ionization time τ_{ion}^{0}. The value of n_H^{∞}, too, is poorly constrained since considerable filtration of interstellar H is expected as it enters the heliosphere. In addition, the solar wind proton density at 1 AU can vary by a factor of 2. Finally, we should observe that equation 4 is valid strictly for a radially symmetric solar wind – it does not take into account latitudinal variation of the wind.

As discussed in Appendix A, the assumption that the pickup ions scatter rapidly onto a bispherical distribution is not completely justifiable. We further disregard acceleration processes (Fermi, drift, etc.) for pickup ions which are a potential source of wave energy. The present approach therefore allows a calculation of an upper limit on the pickup ion induced enhancement of the ambient turbulent magnetic field fluctuation spectrum. We allow for incomplete scattering of the pickup ions and subsequently limited wave generation and proton heating by the pickup population below.

The combination of our assumptions underlying

both the bidirectional distribution and the physical parameters needed for the pickup ion wave source term must render the actual value of $\dot{E}_{PI}$ very uncertain. However, as noted equation 4 provides a maximum estimate (subject to our assumed parameters) of the turbulence levels that interstellar pickup ions can drive. Accordingly, we introduce a parameter $0 \leq f_D \leq 1$ which multiplies the right hand side of equation 4 to give a fraction for the maximum possible magnetic fluctuation energy that can be driven by interstellar pickup ions. We then scan the f_D parameter space of solutions to find appropriate values that are consistent with observations. In this rather crude manner, we hope to subsume into a single parameter f_D the complexities of the pickup ion scattering process, the non-isotropic and temporal character of the solar wind, and the complex physics of neutral H transport throughout the heliosphere. This motivation for f_D is discussed further in Appendix A.

To develop a tractable model for the radial evolution of MHD-scale solar wind fluctuations, we make use of advances in MHD turbulence theory, as well as developments in transport theory for MHD fluctuations in an inhomogeneous medium. The strategy is to employ frameworks that are general enough to accommodate solar wind fluctuations as we currently understand them, while also simplifying the theoretical description as far as possible.

As a first step, we view the fluctuations *locally* as nearly incompressible [*Zank and Matthaeus*, 1992a], strongly nonlinear and homogeneous [*Tu et al.*, 1984; *Zhou and Matthaeus*, 1990]. This will simplify the description of both the transport and the turbulent dynamics. Transport equations for such locally homogeneous incompressible fluctuations, derived using an assumption of scale separation ($\lambda/r \ll 1$), thereby generalizing WKB theory [*Marsch and Tu*, 1988; *Tu and Marsch*, 1993; *Zhou and Matthaeus*, 1990; *Matthaeus et al.*, 1994], have been used to explain various features of solar wind turbulence in recent years. These transport equations involve various correlation functions (up to 16 in number) that can be written in terms of the Elsässer variables $\mathbf{z}_\pm = \mathbf{v} \pm \mathbf{b}$. *Matthaeus et al.* [1994] have shown how these equations simplify greatly for the case of the energy-containing fluctuations, for which detailed spectral information is not needed. *Zank et al* [1996] and *Matthaeus et al* [1996], discuss how considerable further simplification can be employed for application to the outer heliosphere, for which, for example the inequality $U >> V_A$ may be exploited, along with the condition of low or zero net cross helicity ($\mathbf{v}$ and $\mathbf{b}$ uncorrelated).

To describe turbulent evolution and decay, a simplified phenomenological (or, "one-point") theory can be derived for the evolution of the "energy-containing eddies" in a homogeneous turbulent MHD medium [*Dobrowolny et al.*, 1980; *Grappin et al*, 1983; *Hossain et al.*, 1995]. This approach is analogous to the Taylor–von Kármán approach [*Taylor*, 1935; *von Kármán and Howarth*, 1935] for hydrodynamics. A distinguishing feature of the MHD case with a locally uniform mean magnetic field $\mathbf{B}_0$ is the appearance of anisotropy in wavenumber space [*Shebalin et al.*, 1983; *Oughton et al.*, 1994; *Sridhar and Goldreich*, 1994; *Matthaeus et al.*, 1998; *Oughton et al.*, 1998] associated with suppressed spectral transfer in the direction parallel to $\mathbf{B}_0$. For simplicity, we postulate that spectral transfer is of the quasi-2D or nearly "zero frequency" type, usually described by reduced MHD [*Montgomery*, 1982; *Zank and Matthaeus*, 1992b; *Oughton et al.*, 1998; *Kinney and McWilliams*, 1998].

The homogeneous decay phenomenology can be married to the transport formalism in the spirit of a scale-separated expansion [*Marsch and Tu*, 1988; *Zhou and Matthaeus*, 1990; *Matthaeus et al.*, 1994]. Accordingly, after assembly of the above theoretical pieces and imposing the simplifications appropriate to the outer heliosphere [*Zank et al*, 1996; *Matthaeus et al.*, 1996, 1999], the theory takes the form:

$$\frac{dZ^2}{dr} = -\frac{A'}{r}Z^2 - \frac{\alpha}{U}\frac{Z^3}{\lambda} + \frac{\dot{E}_{PI}}{U}, \qquad (5)$$

$$\frac{d\lambda}{dr} = -\frac{C'}{r}\lambda + \frac{\beta}{U}Z - \frac{\beta}{U}\frac{\lambda}{Z^2}\dot{E}_{PI}, \qquad (6)$$

$$\frac{dT}{dr} = -\frac{4}{3}\frac{T}{r} + \frac{2}{3}\frac{m_p}{k_B}\frac{\alpha}{U}\frac{Z^3}{\lambda}. \qquad (7)$$

Note that several constants appear in the equations. These are either fixed by boundary data, determined by our model for shear and pickup driving, or else are either fixed or tightly constrained by the geometry (rotational symmetry) or other properties of the turbulent fluctuations [see, e.g., *Zank et al.*, 1996; *Matthaeus et al.*, 1996]. We discuss these issues presently.

Although equations (5)–(7) are given in steady-state form, they are derived as initial value equations with their temporal variation expressed as an advective derivative. We take $V_{SW} = 400\,\mathrm{km\,s^{-1}}$ to be the (presumed constant) solar wind speed. It then becomes necessary to specify the initial (boundary)

conditions at 1 AU for the magnetic fluctuation energy Z^2_{1AU}, the similarity scale λ_{1AU} and the proton temperature T_{1AU}. The remaining parameters: A', C', α and β, are heavily constrained by rotational symmetry, Taylor–Kármán local phenomenology, and solar wind conditions [*Matthaeus et al.*, 1996; 1999]. We take $A' = -1.1$, $C' = 1.8$, $\alpha = 1$, and $\beta = 1$. $\dot{E}_{PI}$ is the energy injection rate due to pickup ions defined above. The similarity scale λ may be associated with a correlation scale transverse to the mean field [*Batchelor*, 1953] given by $\int_0^\infty R_{NN}(r', 0, 0)\,\mathrm{d}r' \equiv L = \lambda Z^2$ where R_{NN} is the 2-point autocorrelation function for the N-component of magnetic fluctuations. An alternate e-folding definition for λ is that separation distance where $R_{NN}(\lambda^e) = R_{NN}(0)/e$ (where e is the base of natural logarithms 2.718...). A more detailed description of the theory is available [*Matthaeus et al.*, 1999] while Appendix B discusses difficulties in associating the similarity scale with the correlation length. Z^2, λ, and T will be compared to observations in the following section after identification of 1 AU initial conditions.

Lastly, we define the parameters used in the following comparisons to model the driving terms: To model the wind shear and compression, we will vary $C_{shear} + C_{comp}$ in the following analysis. Since the functional forms for shear- and compression-driving are the same in the approximation given by *Zank et al.* [1996] and above, we hereafter refer only to C_{shear} when the sum of both source terms is implied. The pickup energy input scales as $\dot{E}_{PI} \sim f_D v_A U n_H/\tau$, where n_H is the density of interstellar neutrals, and τ is their ionization time. We will adjust the strength of this term by varying f_D below. As an example, if we take $f_D = 0.04$ this would mean that only 4% of the particle energy available for wave production by scattering of the newborn pickup ions from a beam to a bisherical distribution is assumed to be deposited into the flow. A closer examination of this assumption is presented below and in Appendix A.

3. Observations

The theory described above assumes a steady, radially dependent energy injection terms (wind shear and newborn pickup ions) and a constant source boundary for the solar wind and IMF fluctuations. Because the theory assumes $\langle \mathbf{v} \cdot \mathbf{b} \rangle = 0$, we neglect measurements taken in the inner heliosphere ($r < 1$) and by Ulysses which explored the high-latitude wind. We use the NSSDC Omnitape dataset [*King and Papitashvili*, 1994] to provide a baseline for solar wind observations starting well before the launch of the Voyager spacecraft and continuing into the present. The Omnitape measurements are used to normalize

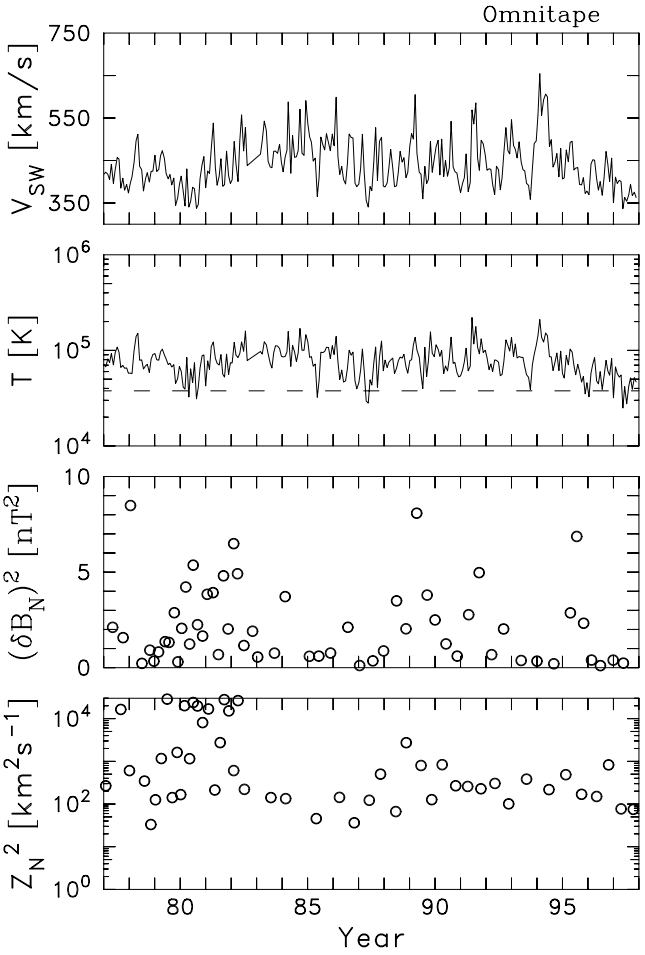

Figure 2. *Top panel:* Solar wind speed taken from hourly averages of interplanetary observations recorded in near-Earth orbit as obtained from the NSSDC Omnitape dataset and averaged over one solar rotation. *Second panel:* Proton temperatures recorded on the same dataset and averaged in the same manner. The dashed line in the middle panel is set at 3.77×10^4 K. *Third panel:* Solar-rotation averages of the IMF fluctuation energy at 1 AU contained within the N component only as derived from 10-hour means and averaged over 50 consecutive subintervals. *Bottom panel:* Solar-rotation averages of the combined magnetic and velocity fluctuation energy in Alfvén units, Z^2.

the Voyager observations in the hope of removing the variability of the solar source.

3.1. Omnitape

Figure 2 shows a series of solar rotation averages of the interplanetary plasma parameters as recorded on the Omnitape dataset from 1977 through 1998. The top panel shows the average wind speed with some evidence of solar cycle effects. It is interesting to note that while solar maximum is expected to bring the greatest number of disturbances, the average wind speed actually decreases during these times and the highest average wind speeds are observed during solar minimum. Variability from one solar rotation to another is a basic feature of these datasets and a good measure of the unpredictability in these numbers as we will be using them. The systematic variability with solar cycle is a good example of the motivation for performing the 1 AU normalization described below. The second panel of Figure 2 shows averages of the proton temperature computed in the same manner, together with the 3.77×10^4 K value taken for the mean proton temperature at 1 AU by *Richardson et al.* [1995] in their analysis of the Voyager 2 proton temperatures. This value appears to be low and the variability seen in the top panel is again present.

The third panel of Figure 2 shows solar rotation averages of the IMF fluctuation energy calculated from 10-hour samples (N component only) over the same period. We use 1-hour averages of the N component only, which is generally free of sector crossings, compute a 10-hour mean and a resulting variance, and average over 50 such sequential and nonoverlapping 10-hour periods to obtain each point in this panel. Subintervals with variances larger than the magnitude of the mean are discarded under the assumption that they are contaminated by shocks and other transient signals. A high degree of variability is seen in association with the 11-year solar cycle. The bottom panel shows solar rotation averages of Z^2 as computed for the N-component only. Variability is seen from 10^2 to $10^3\,\mathrm{km^2 s^{-2}}$ with some anomalously high values around 1980; values of $Z^2 = 200$ to $400\,\mathrm{km^2 s^{-2}}$ are most typical. It is essential that we take into account the observed variability of 1 AU parameters when examining IMF power and proton temperatures in the outer heliosphere [*Burlaga and Ness*, 1993; *Zank et al.*, 1996], or temporal variations of the solar source may mask the true radial dependence of the data.

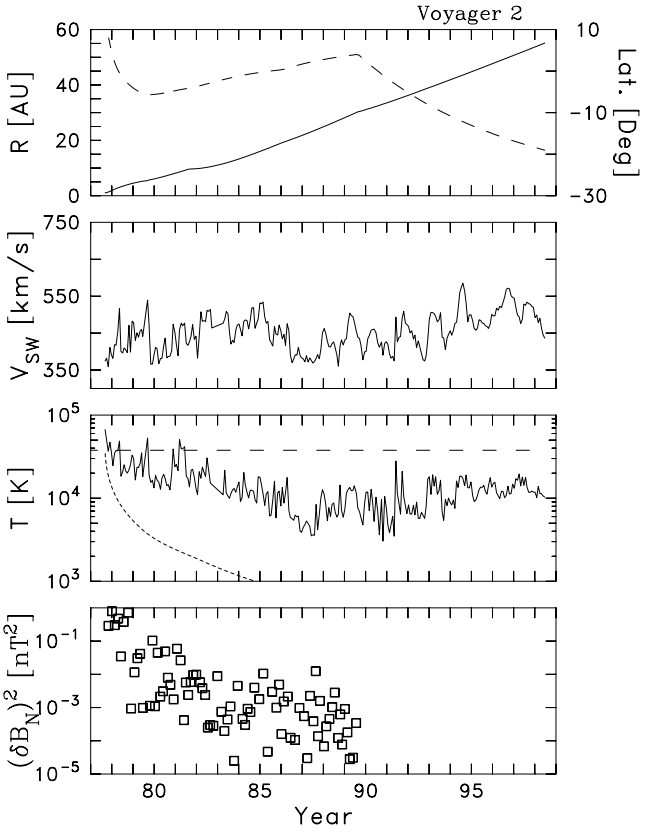

Figure 3. *Top panel:* Solar-rotation averages of the heliocentric distance (solid) and heliographic latitude (dashed) of the Voyager 2 spacecraft from launch until late in 1998. *Second panel:* Solar-rotation averages of the solar wind speed. *Third panel:* Proton temperature averaged over approximate solar rotations shows an end to the temperature decline starting ~1990 followed by a slow increase in proton temperature while the spacecraft remains at relatively low latitude for over 5 years. Dotted line is the adiabatic expansion prediction $r^{-4/3}$. *Bottom panel:* IMF fluctuation energy contained within the N component only (bottom panel) as computed for hourly samples from a 10-hour mean and averaged over 50 consecutive 10-hour intervals. Analysis is limited to pre-1990 observations when spacecraft noise is not yet a significant problem.

3.2. Voyager 2

Figure 3 was computed in a manner similar to Figure 2, except for the additional top panel showing the spacecraft's heliocentric distance (solid curve) and heliographic latitude (dashed curve). Note that

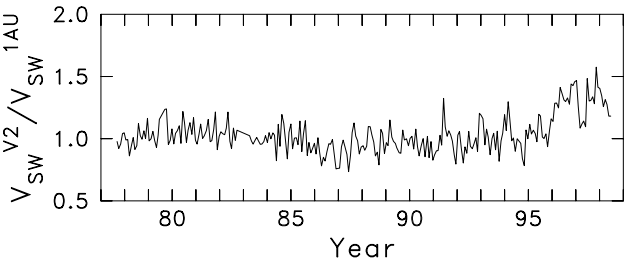

Figure 4. A simple time-lagged ratio of the solar wind speed observed by Voyager 2 (averaged over one solar rotation) vs. the same for the Omnitape dataset. The time lag uses the average solar wind speed observed for the particular subinterval of Voyager 2 data and the observed spacecraft location. Note that the upturn in solar wind speed does not occur until ~1995, when the spacecraft latitude becomes large.

the spacecraft remains within 10° of the heliographic equator until after mid-1993. The second panel shows the average wind speed, which again shows some degree of variability in association with the solar cycle. The average wind speed remains below 550 km s^{-1} except for a few isolated solar rotations, suggesting that the spacecraft is sampling approximately no more of the high-latitude wind than is seen in the Omnitape dataset.

The third panel in Figure 3 shows the variability of the ambient proton temperature with a systematic decrease until ~1988 at approximately which point the temperature levels off and begins a slow and highly variable increase. (The 1 AU value given by Richardson et al. is again plotted for reference as the dashed line.) This panel also shows the $r^{-4/3}$ behavior of the proton temperature predicted under the assumption of purely adiabatic expansion. It is clear from the comparison of the observations with this prediction that energy is supplied to the plasma in the form of heat [*Richardson et al.*, 1995]. This is made more dramatic by the observed increase in proton temperature beginning in 1988.

The bottom panel in this figure shows the generally decreasing IMF fluctuation energy as the spacecraft moves to greater heliocentric distance in keeping with the analysis of *Zank et al.* [1996] and *Matthaeus et al.* [1999]. Analysis of the IMF data stops before spacecraft noise contaminates the results.

Figure 4 shows an analysis of the average wind speed observed by Voyager 2 divided by a time lagged average of the Omnitape observations. The time lag is computed to be consistent with the advection time from 1 AU to the spacecraft. Note that the resulting normalized wind speed is remarkably constant until ~1995, at which point the average wind speed observed by the Voyager 2 spacecraft begins a steady increase relative to the Omnitape observations. This is a full 7 years after the leveling of the Voyager proton temperatures, which strongly suggests that the Voyager observations before this point are not the result of observations of the high latitude solar wind, but, in fact, result from enhanced heating of the interplanetary protons. At this time (the beginning of 1995) the Voyager 2 spacecraft is at 45 AU. High-speed winds at 1 AU are observed to be generally hotter than the surrounding plasma [*Barnes*, 1979] and Ulysses observations at high latitudes and in high-speed wind show similarly consistent high temperatures [*McComas et al.*, 2000]. The normalized Voyager 2 temperatures (Figure 3) do not rise significantly or dramatically as the normalized wind speed (Figure 4) rises and the spacecraft latitude decreases beyond approximately −15° after 1995.

We now apply the theory of turbulent heating and transport outlined in Section 2. We do so with a sequence of three plots that explore the parameter space available to the theory and examine the ability of each parametric variation to fit the observed behavior of the data.

Figure 5 shows the three analyses of solar wind measurements we will need to test this theory. The IMF fluctuation energy of the N component (top panel) computed as above and normalized by the time lagged analysis of the Omnitape IMF dataset analyzed in the same fashion is compared with three different parameterizations of the initial conditions for the solar wind at 1 AU. The solid curve shows the solution for $Z_{1AU}^2 = 350\,\mathrm{km^2 s^{-2}}$, $\lambda_{1AU} = 0.03\,\mathrm{AU}$, and $T_{1AU} = 60000\,\mathrm{K}$. The curve of long dashes represents the solution for $Z_{1AU}^2 = 400\,\mathrm{km^2 s^{-2}}$, $\lambda_{1AU} = 0.025\,\mathrm{AU}$, and $T_{1AU} = 40000\,\mathrm{K}$. The curve of short dashes represents the solution for $Z_{1AU}^2 = 250\,\mathrm{km^2 s^{-2}}$, $\lambda_{1AU} = 0.03\,\mathrm{AU}$, and $T_{1AU} = 90000\,\mathrm{K}$. These initial conditions are well within the range shown in Figure 2. In all cases we take $C_{shear} = 2$ and the pickup ion source is turned off ($f_D = 0$). The theoretical predictions for the magnetic energy are virtually identical and in good agreement with the observations. The predictions for the magnetic correlation length are also nearly identical and seen to be in good agreement with the observations with some underestimation of

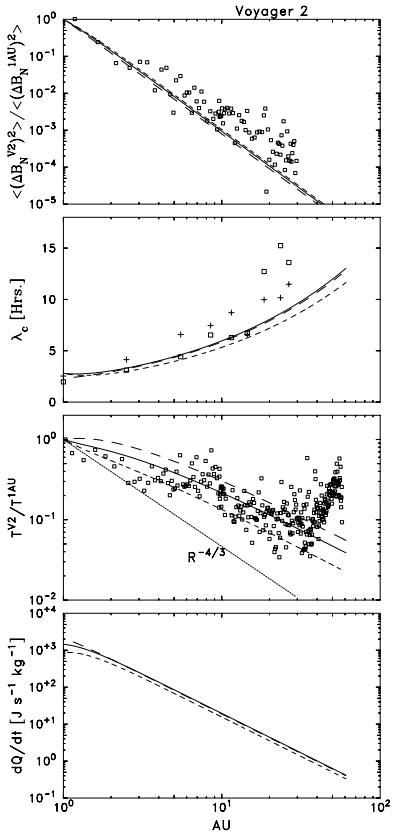

Figure 5. *Top panel:* Observed IMF fluctuation energy in N component normalized by 1 AU observations (□) plotted vs. the theoretical predictions for turbulence driven by wind shear alone. Three different sets of initial conditions are chosen as described in the text. *Second panel:* Observed correlation length for the N component computed by integration method (□) and e-folding definition (+) plotted vs. theoretical predictions for same three sets of initial conditions. Values for 1 AU are computed from the NSSDC Omnitape dataset. *Third panel:* Observed proton temperature normalized by 1 AU observations (□) plotted vs. the theoretical predictions. Dotted line is the non-dissipative prediction of adiabatic expansion $r^{-4/3}$. *Bottom panel:* Specific heating rates as predicted by the model for the three cases shown above. Note that while the heating rates of the three parameterizations are nearly identical, the initial conditions assume different values for T_{1AU} so that different fractional temperature changes are obtained for the same heat input as demonstrated in the above panel.

the observations at the larger heliocentric distances.

The fact that the three parameterizations yield similar predictions for the magnetic energy is not unexpected. In fact, the WKB prediction is also nearly identical to the observed results [*Roberts et al.*, 1990; *Zank et al.*, 1996]. This is because the theory assumes that whatever energy is added to the IMF fluctuations is ultimately dissipated by spectral transfer to the small scales. An enhanced spectrum leads to enhanced cascade and an increase in dissipation so that a wide range of parameterizations lead to very nearly identical magnetic energy levels. The same cannot be said of the proton temperature since heating is the end result of the turbulent energy cascade. The proton population can accumulate significantly distinct levels of thermal energy depending on the heating rate. This is perhaps the key discriminator for solar wind heating models.

The second panel of Figure 5 shows the measured correlation length for the N component computed from the integration definition (squares) and e-folding definition (+) described in section 2. Values for the correlation length are computed using 120 hour maximum lags for individual solar rotations. The resulting estimates are then averaged over 3 AU. Values for 1 AU are obtained from the Omnitape dataset using the same analysis method. Theoretical predictions for the correlation length derived from the same solutions of equation 6 are also plotted using the same solid and dashed line convention as above. Again, the agreement is generally good with the theoretical predictions showing nearly identical results and slightly underestimating the observations.

The third panel of Figure 5 shows the measured proton temperature normalized by the time lagged analysis of the Omnitape dataset. The observations are consistently bracketed by the 3 theoretical formulations until the most recent observations beyond ~40 AU. Consideration of solar cycle effects fails to resolve the clear difference between the observations and the predictions of simple adiabatic expansion given by the $r^{-4/3}$ dashed line. Evidently wind shear alone provides a good description for the proton temperature out to ~40 AU. From this point outwards the ambient protons are systematically hotter than the wind-shear driven theory predicts.

There appears to be a significant rise in the observed temperature beyond 40 AU and it is unclear from this plot whether the observed behavior is the result of enhanced heating at this distance or perhaps the result of latitudinal effects (recall that Voyager is

observing higher wind speeds than Omnitape at this time). We will return to this question below.

The bottom panel of Figure 5 shows the predicted specific heating rates derived from the theory for the three parameterizations described above. Because all three solutions possess the same parameterizations for the driving terms (C_{shear}, C_{comp} and f_D), the specific heating rates are nearly identical with the variation due only to the initial conditions (recall that this is a nonlinear theory). The nearly identical specific heating rates still produce significant differences in the predicted normalized temperatures shown in the above panel largely because these are normalized to 1 AU values and the fractional temperature change for approximately equal heat input varies with T_{1AU}.

In addition to possible sensitivity to initial conditions, the theory parameterizes the driving terms for wind shear and pickup ions. We next examine the sensitivity of these results to parametric variation of the driving term due to wind shear C_{shear}.

Figure 6 shows the result of this variation for three different values of $C_{shear} = 1$ (short dashes), 2 (solid curve), and 3 (long dashes). In each case we use the initial conditions: $Z^2_{1AU} = 350\,\mathrm{km^2 s^{-2}}$, $\lambda_{1AU} = 0.03\,\mathrm{AU}$, and $T_{1AU} = 60000\,\mathrm{K}$ which is the same initial condition shown in the solid curve in Figure 5. Again, the magnetic energy (top panel) shows almost identical predictions that consistently underestimate the observed magnetic fluctuation energy. Enhancing the driving term separates the predicted similarity lengthscales (second panel) so that the more aggressively the turbulence is driven the greater the prediction underestimates the observed correlation lengths. The proton temperature (third panel) is again bracketed nicely by the range of driving terms; however, the theory fails to account for the upturn in the temperature observed beyond 40 AU. Beyond this limitation neither parameterization of the driving term shows significant disagreement with the observations. The predicted heating rates are shown in the bottom panel. Since C_{shear} now varies it is not surprising that the specific heating rates vary, too, and this accounts for the different temperatures predicted by the three solutions.

Leamon et al. [1999] examined magnetic fluctuation spectra at 1 AU. By employing a model for magnetic dissipation based on kinetic Alfvén waves they offered an estimate for the proton heating rate to be $3.7 \times 10^{-17}\,\mathrm{J\,s^{-1}m^{-3}}$, which was 58% of the total dissipation they inferred. The remaining energy was argued to be go into electron heating. For the spe-

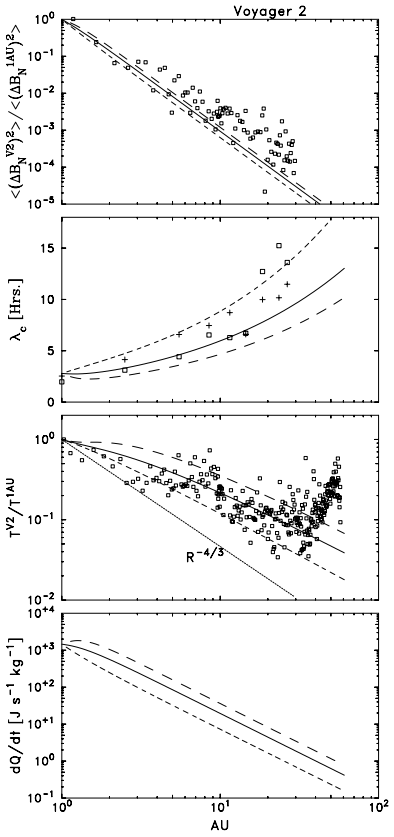

Figure 6. *Top panel:* Observed IMF fluctuation energy in N component normalized by 1 AU observations (□) plotted vs. the theoretical predictions for turbulence for 3 different parameterizations of the shear driving term. Three different sets of initial conditions are chosen as described in the text. *Second panel:* Observed correlation length for the N component computed by integration method (□) and e-folding definition (+) plotted vs. theoretical predictions for same three sets of initial conditions. Values for 1 AU are computed from the NSSDC Omnitape dataset. *Third panel:* Observed proton temperature normalized by 1 AU observations (□) plotted vs. the theoretical predictions. Dotted line is the non-dissipative prediction of adiabatic expansion $r^{-4/3}$. *Bottom panel:* Specific heating rates as predicted by the model for the three cases shown above. Note that while the three parameterizations use the same value of T_{1AU}, the heating rates are changed in response to the 3 values of C_{shear} leading to 3 different temperature curves in the above panel.

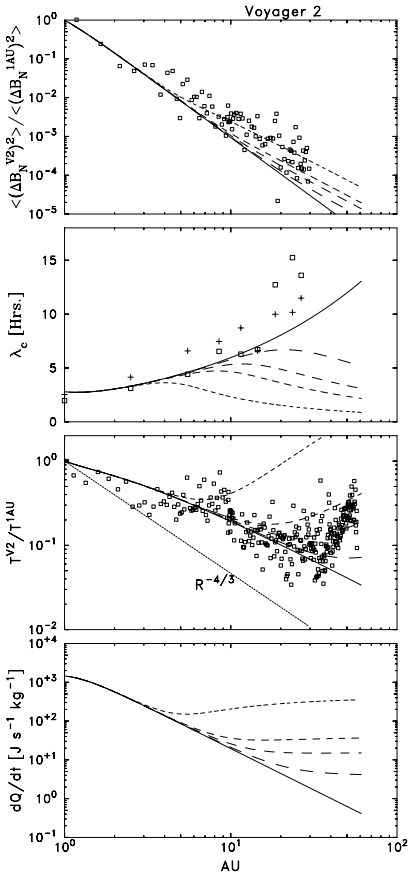

Figure 7. *Top panel:* Observed IMF fluctuation energy in N component normalized by 1 AU observations (□) plotted vs. the theoretical predictions for turbulence for 5 different parameterizations of the driving by pickup ions term. Five different sets of initial conditions are chosen as described in the text. *Second panel:* Observed correlation length for the N component computed by integration method (□) and e-folding definition (+) plotted vs. theoretical predictions for same five sets of initial conditions. Values for 1 AU are computed from the NSSDC Omnitape dataset. *Third panel:* Observed proton temperature normalized by 1 AU observations (□) plotted vs. the theoretical predictions. Dotted line is the non-dissipative prediction of adiabatic expansion $r^{-4/3}$. *Bottom panel:* Specific heating rates as predicted by the model for the three cases shown above. Enhanced heating due to pickup ions leads to nearly constant specific heating rates in the outer heliosphere.

cific interval they modelled the proton density was $4.54\,\mathrm{cm}^{-3}$, which translates the above into a specific heating rate of $0.48 \times 10^4\,\mathrm{J\,s^{-1}\,kg^{-1}}$. This is approximately $3\times$ the value given by the three solutions shown in this figure and $5\times$ the lowest valued solution shown in Figure 5. There is as yet no indication whether the prediction of Leamon et al. will be sustained when other intervals are modelled in the same fashion. Since wind shear and compressive heating require some time to reach peak efficiency, and since 1 AU observations are a function of inner heliospheric dynamics, it is likely that 1 AU spectra may yield different results than the fitting of Voyager observations will provide. Leamon et al. do argue that their results agree more nearly with the inferred heating rates derived from Helios observations [*Freeman*, 1988] than with Voyager observations [*Richardson et al.*, 1995].

Lastly for the Voyager 2 dataset, we examine the possible role of pickup ions in driving interplanetary turbulence in the outer heliosphere. Figure 7 shows a variation of the pickup ion source term $f_D = 0.0$, 0.01, 0.04, 0.10, and 1.0 where progressively higher values of f_D are represented by shorter dashed lines. In all cases we use the same initial conditions used in Figure 6 but with a slightly elevated initial temperature: $Z^2_{1AU} = 350\,\mathrm{km^2 s^{-2}}$, $\lambda_{1AU} = 0.03\,\mathrm{AU}$, and $T_{1AU} = 70000\,\mathrm{K}$ and we use the wind shear driving term $C_{shear} = 2$.

The addition of the pickup ion term, which is active outside the ionization cavity and generally at larger heliocentric distances than where the shear driving term contributes, introduces three significant changes in the results shown. First, the predicted magnetic fluctuation energy is enhanced and the five values of f_D can be seen to produce five distinct predictions for the magnetic energy that offer better agreement with the observations than obtained previously (top panel). Second, the predictions for the similarity lengthscales now diverge quite severely from the computed correlation lengths of the fluctuations (second panel). The discrepancy between theory and observation is a clear weakness in this version of the theory. This discrepancy may be due to the theory itself in the way that driving by pickup ions influences the similarity scale, to our association of the similarity scale λ with the correlation scale λ_c, to problems inherent in any measurement of the correlation scale, or to a combination of these possibilities (see Appendix B). Third, the predicted proton temperature can now be seen to possess a distinct upturn in the outer heliosphere which appears to be in better keeping with

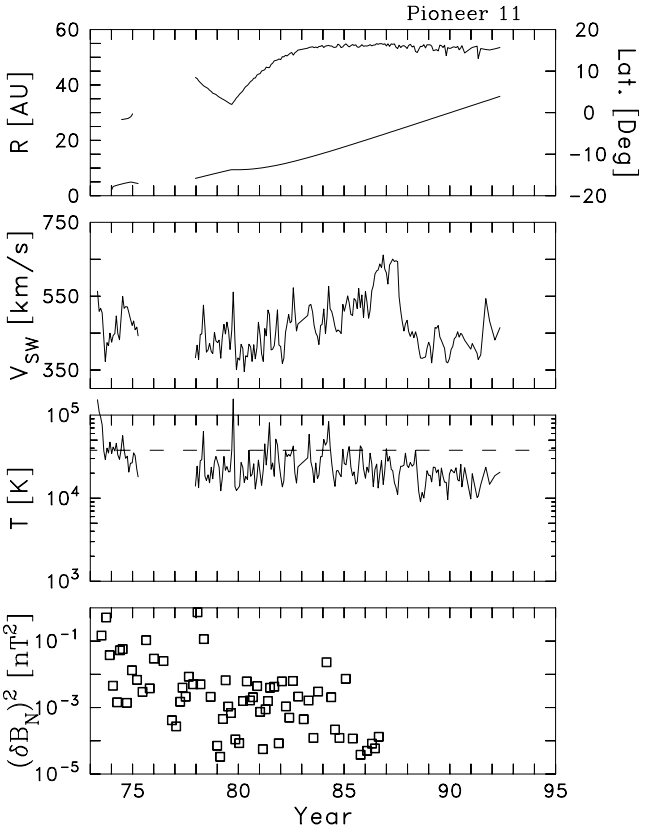

Figure 8. *Top panel:* Solar-rotation averages of the heliocentric distance (solid) and heliographic latitude (dashed) of the Pioneer 11 spacecraft from launch until late in 1992. *Second panel:* Solar-rotation averages of the solar wind speed showing a marked increase starting possibly as early as 1980 and peaking in 1987. *Third panel:* Proton temperature shows a remarkably flat form that drops only slightly from 1985 onward. Comparison with Voyager 2 observations suggests that the relatively rapid rise in heliographic latitude may account for the systematic rise in wind speed and sustained level of ambient proton temperature. *Bottom panel:* Solar-rotation averages of the IMF fluctuation energy contained within the N component only.

the observations (third panel). Values of $f_D < 0.1$ give the best agreement with the observations. The stronger driving due to with $f_D > 0.1$ provides too much dissipation and excessive proton temperatures for these values of initial conditions and wind shear driving. The bottom panel shows the specific heating rates for these five solutions with the most striking result being that the addition of the pickup ion term leads to asymptotically constant specific heating rates in the outer heliosphere.

In spite of the improved agreement with the observations offered by the pickup ion driving term, it would seem that there is a precipitous rise in temperature beyond ∼40 AU that is too abrupt to be matched by the predictions. This occurs at approximately the same time that the spacecraft is moving below −10° of heliographic latitude (∼1995) and when the spacecraft is getting well into solar minimum conditions. Since solar minimum implies the establishment of a consistent high/low wind speed source pattern at the sun in association with high/low source latitudes, it seems likely that Voyager is at this time sampling high-latitude and high-speed wind sources that are separate from the observations recorded on the Omnitape for near-Earth spacecraft within the ecliptic plane. This suggestion is supported by the upturn in the normalized wind speed at this time shown in Figure 4. Therefore, we now examine Pioneer 11 observations as they provide a separate and independent trajectory into the high-latitude wind that may confirm or refute the suggestion that the observed behavior of the Voyager temperatures beyond ∼40 AU are linked to spacecraft latitude.

3.3. Pioneer 11

The precipitous rise in the normalized proton temperature observed by the Voyager 2 spacecraft from about 40 AU onward and as the spacecraft descends below -10° heliographic latitude may be the result of increased sampling of the fast, hot, high-latitude wind observed by the Ulysses spacecraft [*McComas et al.*, 2000]. We can look for possible confirmation of this interpretation by examining the Pioneer 11 dataset. The Voyager 1 plasma instrument failed shortly after its encounter with Saturn, making high-latitude measurements unavailable from that spacecraft and the Pioneer 10 spacecraft has not achieved the high latitudes needed for this study. Figure 8 shows the basic Pioneer 11 observations computed in the same manner as was used in the Voyager analysis shown in Figure 3. The spacecraft climbed rapidly to +15° north latitude after its encounter with Saturn in 1980. There is an unexplained data outage of the plasma instrument from day 102 of 1975 until day 341 of 1977. With the spacecraft latitude increasing the observed mean wind speed starts to increase as early as 1980 with the same short-term variability seen in the Voy-

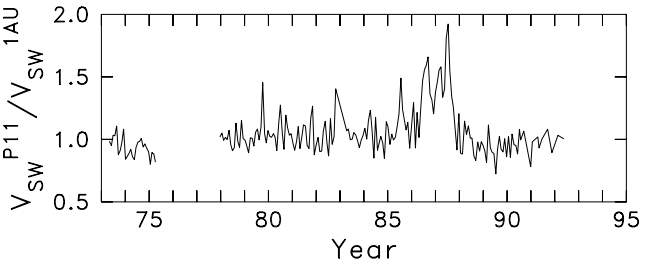

Figure 9. A simple time-lagged ratio of the solar wind speed observed by Pioneer 11 and averaged over one solar rotation and the same for the Omnitape dataset. The time lag uses the average solar wind speed observed for the particular subinterval of Pioneer 11 data and the observed spacecraft location. This analysis seems to suggest that the rise in wind speed relative to the 1 AU in-ecliptic observations starts in 1985 when the spacecraft is at 16° north latitude and the solar cycle is in solar minimum. The subsequent decline in average wind speed at this latitude may be associated with the onset of solar maximum.

ager dataset, and continues until late in 1987 when the wind speed falls precipitously. Throughout the climb in wind speed the proton temperature is observed to be remarkably constant when compared with the Voyager 2 observations and this is probably due to the increasing spacecraft latitude. The bottom panel of the figure shows the observed magnetic fluctuation energy in the N component to which we return below.

Figure 9 shows the average Pioneer 11 wind speed normalized by lagged Omnitape observations in the same manner as was used in Figure 4. This analysis seems to reduce the interval of high wind speed observed by Pioneer 11 to the period beginning in 1985, which suggests that the apparently elevated wind speed in Figure 8 from 1980 to 1985 may be related to the solar cycle. The precipitous decrease in the wind speed, to levels consistent with Omnitape observations, that occurs late in 1987 is confirmed here. It would seem that solar cycle effects at this time have permitted both Pioneer and Omnitape to observe similar percentages of high wind-speed intervals, thereby negating any latitudinal effects in the observed temperature at this time.

Figure 10 shows the analysis of the Pioneer 11 dataset using the same analysis method employed above and compares the Pioneer observations with

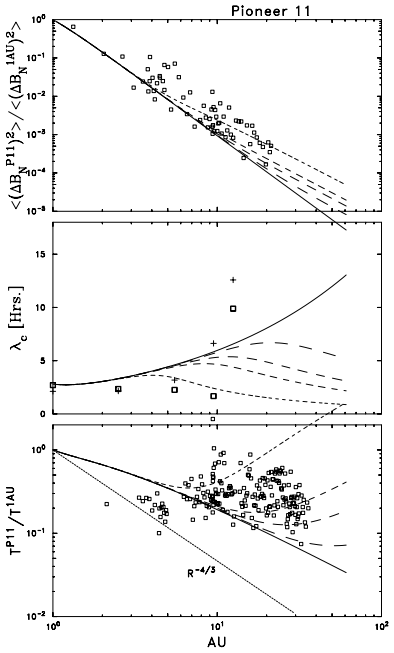

Figure 10. Pioneer 11 analysis. *Top panel:* Observed IMF fluctuation energy in N component normalized by 1 AU observations (□) plotted vs. the theoretical prediction. Parameterization of the turbulence predictions are the same as shown in Figure 7. *Middle panel:* Observed correlation length for the N component computed by integration method (□) and e-folding definition (+) plotted vs. theoretical prediction (solid). Values for 1 AU are computed from the NSSDC Omnitape dataset. *Bottom panel:* Observed proton temperature normalized by 1 AU observations (□) plotted vs. theoretical prediction. Dotted line is the adiabatic expansion prediction $r^{-4/3}$.

the predictions of the transport theory. The same parameterizations of the theory as used in Figure 7 are used here. The magnetic energy agrees well with the theory, but the correlation lengths continue to provide striking disagreement beyond ∼10 AU. Disagreement between the correlation lengths computed from the Voyager and Pioneer datasets are not understood at this time. We take this up in Appendix B. The observed proton temperatures are in good agreement with the theory until about 20 AU when they systematically exceed the $f_D = 0$ prediction. Excitement of magnetic energy and heating of the ambient proton population beyond ∼20 AU are well characterized by $f_D \gtrsim 0.1$. However, 20 AU corresponds to the

high wind-speed period of the Pioneer observations. The observed proton temperatures remain in keeping with the theoretical predictions when the observed wind speed returns to Omnitape levels. This would seem to confirm the general applicability of the theory. The suggestion that the departure of the Voyager observations from the theoretical predictions observed during recent years is most likely interpreted as a latitudinal effect rather than a disagreement with the theory would seem to remain unanswered except for the unexplained rapidity of the rising temperatures in recent years.

4. Summary

We have presented a test of a recent model for the turbulent heating of the interplanetary plasma. Heating by pre-existing fluctuations [*Schwartz et al.*, 1981] is insignificant in comparison with the energy that spectral transport can deliver from the large-scale fluctuations. The large-scale wind shear and magnetic waves generated by the scattering of suprathermal pickup ions constitute a large energy source available to the dissipation processes. The nonlinear processes inherent in the turbulent evolution of the fluid transport the low-frequency energy to smaller spatial scales where resonant and nonresonant processes can dissipate the energy, thereby heating the background ions. The details of the dissipation process are not important to this model (see *Leamon et al.* [1998a; 1998b; 1999; 2000] for discussions of IMF dissipation processes).

We have argued and attempted to demonstrate that solar wind protons undergo significant heating as the wind advects outward and that the heating continues as far as Voyager observations extend. Solar wind expansion is far from adiabatic. In so demonstrating, we have attempted to take into account solar variability using the Omnitape dataset and changing heliographic latitude using both Omnitape and the Pioneer 11 observations. We have shown that a relatively wide range of initial values representing solar wind conditions at 1 AU in combination with a range of parameters describing interplanetary turbulence conditions can reproduce the observations. This is a nonlinear model and it must be admitted that extreme solutions can be generated, but we have attempted to demonstrate that a wide range of parameterizations lead to general agreement with the observed behavior. Further refinement of the applicable parametric range of this model is probably not possible and is not warranted given the variability of solar wind conditions. However, further refinement of the model itself is possible and efforts to explain the clear disparity between the predicted similarity scale and the observed correlation scale of the turbulence are ongoing. We are presently engaged in an effort to apply a suitable extension of this model to the high-latitude observations of the Ulysses spacecraft where nonzero correlation between the magnetic and velocity fluctuations must be taken into account.

Lastly, we note that *Leamon et al.* [1999] predicts that dissipation of magnetic fluctuations in the interplanetary medium will lead to a significant degree of heating of the ambient electron population at 1 AU. In their theory an approximately equal amount of heat is injected into the thermal proton and electron populations. The theory discussed here omits electron heating, but it appears clear from the range of parameters presented that a similar measure of electron heating could be permitted without significantly altering the predictions for the magnetic fluctuation energy or similarity scale. In closing, it appears unlikely that consideration of electron heating will significantly alter the conclusions reached here.

Appendix A: Variation of Pickup Ion Source

Neutral atoms from the local interstellar medium flow slowly ($\approx 20\,\mathrm{km s^{-1}}$ for neutral hydrogen) into the heliosphere where some are ionized, by either solar EUV radiation or charge exchange with solar wind protons, to become pickup ions. Self-generated and in situ waves act to scatter the pickup ions in pitch angle toward a nearly isotropic bispherical distribution [*Lee and Ip*, 1987; *Johnstone et al.*, 1991; *Williams and Zank*, 1994; *Isenberg and Lee*, 1996]. Quasi-linear calculations by *Lee and Ip* [1987] predicted that the time scale for isotropization of new born pickup ions should be short compared to the ionization time scale.

Virtually all theoretical work addressing interstellar pickup ions in the solar wind over the last ~25 years has assumed that pickup ions generate significant levels of magnetic field fluctuations. The fluctuations were then assumed to scatter the pickup ions rapidly, so ensuring that the pickup ion distribution was essentially isotropic in the solar wind frame and co-moving with the solar wind. Concerns about the above picture for the pickup of interstellar ions, wave generation and scattering had begun to emerge in the early to mid 1990's when a concerted effort by

several groups failed to find definitive observational evidence for wave generation by pickup ions in the outer heliosphere. While this work is largely unpublished (see *Zank* [1999] for a summary), the few events interpreted to date in terms of pickup ion-driven waves, identified as enhancements of magnetic fluctuation spectra near the ion cyclotron frequency, all occurred during periods when the large-scale interplanetary magnetic field IMF was quasi-radial [*Smith et al.*, 1994; *Murphy et al.*, 1995, 1998; *Intriligator et al.*, 1996; *Zank*, 1999].

These concerns were reinforced when *Gloeckler et al.* [1995] presented results from a 30 day integration of pickup ion protons by the Solar Wind Ion Composition Spectrometer (SWICS) on Ulysses over the south polar coronal hole which showed significant anisotropies in the observed pickup ion distribution; in particular, pickup ions in the sunward hemisphere of particle velocity phase were far more numerous than anti-sunward ions, with radial anisotopies exceeding 50%. Moreover, the observed pickup ion spectra appeared to be most anisotropic during periods when the IMF was quasi-radial and almost isotropic during those periods when the IMF and the radial solar wind were oriented at angles $\gtrsim 45°$ to each other [*Mobius et al.*, 1995]. These observations suggest that pickup ions experience great difficulty scattering into the anti-sunward hemisphere of velocity phase space when the average magnetic field is quasi-radial. Obviously, if the IMF is highly oblique to the radial direction, the induced cyclotron motion of the pickup ion will populate the anti-sunward hemisphere of phase space within a gyroperiod. In a quasi-radial IMF, if transport in particle pitch angle is slow compared to the ionization time, a sunward anisotropy in the pickup ion distribution must occur. Furthermore, as noted by *Isenberg* [1997], if the scattering rate is slow, substantial adiabatic cooling of the pickup ions will have occurred before they reach the sunward hemisphere, resulting in a particle energy spectrum which falls with increasing energy as it approaches the expected cutoff velocity at $\nu = 2V_{SW}^R$ (where V_{SW}^R refers to the radial component of the solar wind speed). Such spectra were reported by *Mobius et al.* [1995] for pickup helium.

The difficulty in identifying enhancements in local IMF spectra that might be associated with waves driven by pickup ions [*Smith et al.*, 1994; *Murphy et al.*, 1995; *Intriligator et al.*, 1996], even during periods when pickup ions were observed in the quasi-radial IMF within the ionization cavity, suggest that the wave growth rate $\Gamma_{obs} \approx 0$ much of the time. Such low effective growth rates would be consistent with the observed anisotropic pickup ion spectra. The observations stand in contrast to the predictions of quasi-linear theory and/or the bispherical distribution model (our equation 4). *Zank and Cairns* [2000] have attempted to resolve this observational puzzle by observing that the locally defined mean IMF is changing continually. This holds most strongly for the polar magnetic field which is quasi-radial on large-scales, but changing continually due to large-scale fluctuations. However, the near-ecliptic IMF observations can also demonstrate large swings toward the radial direction [*Smith and Bieber*, 1993]. *Zank and Cairns* [2000] suggest that these variations in field direction engender spatial and temporal variations in the distributions of pickup ions that can lead to the wave growth varying in a stochastic manner. They develop a stochastic growth theory (SGT) model for MHD waves driven by pickup ions, calculating the mean, variance, and characteristic time scales of the pickup ion generated wave growth rate in a quasi-radial IMF, so as to explicitly justify why the wave growth should be stochastic.

A primary conclusion to emerge from the study of *Zank and Cairns* [2000] is that the dynamical character of the IMF prevents the formation of statistically steady-state pickup ion driven wave enhancements in the magnetic fluctuation spectra. The main parameter controlling the frequency of wave enhancements is the variance in the orientation of the fluctuating IMF about the mean field. They show that even were the mean field radial, a large standard deviation from the radial direction in the local IMF fluctuations on the scale of the correlation length would lead to very little effective wave growth.

In order to model this and related physics, we have used the multiplicative factor f_D to modify the magnetic energy introduced by the scattering of interstellar pickup ions.

Appendix B: Correlation Lengths

The theory we present fails to adequately reproduce the observed behavior of the measured correlation lengths, particularly beyond ~10 AU. There are potentially several reasons for this. First, the theory can be extended to better account for the effects of pickup ions on the similarity scale λ and this effort is underway. The resulting equations are significantly more complicated that those presented here and have

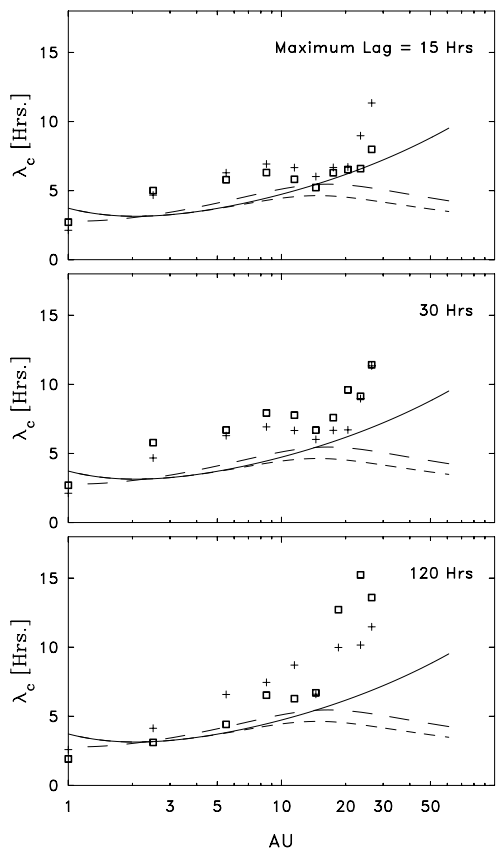

Figure B1. A test of the stability and reproducibility of the measured magnetic correlation lengths as a function of maximum lag. The solid curve and short dashed curve are derived from the theoretical predictions with $Z^2_{1AU} = 250\,\mathrm{km^2 s^{-2}}$, $\lambda_{1AU} = 0.04\,\mathrm{AU}$, and $T_{1AU} = 70000\,\mathrm{K}$. The pickup ion efficiency parameter varies with $f_D = 0$ (solid curve) and $f_D = 0.04$ (short dashes). The long dashed curve is generated using $Z^2_{1AU} = 650\,\mathrm{km^2 s^{-2}}$, $\lambda_{1AU} = 0.03\,\mathrm{AU}$, and $T_{1AU} = 40000\,\mathrm{K}$ with $f_D = 0.04$.

been omitted in this simpler comparison.

Second, the theory derives the evolution of the similarity scale that controls the spectral cascade and we associate this quantity with the correlation length, λ_c. This association is not uncommon [e.g., *Matthaeus et al.*, 1996] and may be quite reasonable as λ_c is a measure of the energy containing scales. However, the association is not required or exact.

Third, we must acknowledge that measurements of magnetic fluctuation correlation lengths are unavoidably complicated by the difficulty in separating low-frequency power due to interplanetary fluctuations and the very large power contained in features that are most credibly attributed to solar sources. The latter is expected to produce long-lag correlations of either positive or negative sign that significantly alter the computed correlation length [*Matthaeus et al.*, 1999]. For instance, Figure B1 shows that as the correlation function is computed out to longer lags the correlation length is extended with that function. This is in part due to the increasing contribution of power associated with very large structures on the scales up to and including several days. It is a highly subjective matter of opinion as to what lengthscales should be used in this analysis. Whatever scales are chosen, the data analysis fails to record the downturn in the correlation lengths predicted by the theory as the result of interstellar pickup ions. We also take this opportunity to show several more solutions for the predicted similarity scale λ.

Acknowledgments. This work was supported by the Voyager program under JPL contracts 959167 to the BRI/UD and 959203 to MIT. Additional support was provided by the NASA Delaware Space College Grant and NASA grants NAG5-6570, NAG5-7164, NAG5-8134 (Sun-Earth Connection Theory Program) and NAG5-6469 and NSF grant ATM-0072810 to the BRI/UD. Support for Sean Oughton is provided by UK PPARC grant PPA/G/S/1999/00059 and by NASA grant NAG5-8134. The authors thank the NSSDC and the Principal Investigators of the Pioneer 11 spacecraft for providing those datasets.

References

Barnes, A., Hydromagnetic waves and turbulence in the solar wind, in *Solar System Plasma Physics*, Vol. 1, edited by E. N. Parker, C. F. Kennel, and L. J. Lanzerotti, pp. 249–319, North-Holland, New York, 1979.

Batchelor, G. K., *The Theory of Homogeneous Turbulence*, Cambridge Univ. Press, New York, 1953.

Belcher, J. W., and L. Davis Jr., Large-amplitude Alfvén waves in the interplanetary medium, 2, *J. Geophys. Res.*, *76*, 3534–3563, 1971.

Burlaga, L. F., and N. F. Ness, Radial and latitudinal variations of the magnetic field strength in the outer heliosphere, *J. Geophys. Res.*, *98*, 3539–3549, 1993.

Coleman, P. J., Jr., Hydromagnetic waves in the interplanetary plasma, *Phys. Rev. Lett.*, *17*, 207–211, 1966.

Coleman, P. J., Jr., Turbulence, viscosity, and dissipation in the solar wind plasma, *Astrophys. J.*, *153*, 371–388, 1968.

Dobrowolny, M., A. Mangeney, and P. Veltri, Properties of magnetohydromagnetic turbulence in the solar wind,

Astron. Astrophys., *83*, 26–32, 1980,

Freeman, J. W., Estimates of solar wind heating inside 0.3 AU. *Geophys. Res. Lett.*, *15*, 88–91, 1988.

Gazis, P. R., Pioneer and Voyager observations of solar cycle variations in the outer heliosphere, *Geophys. Res. Lett.*, *21*, 1743–1746, 1994.

Gazis, P. R., and A. J. Lazarus, Voyager observations of solar wind proton temperature: 1–10 AU, *Geophys. Res. Lett.*, *9*, 431–434, 1982.

Gloeckler, G., N. A. Schwadron, L. A. Fisk and J. Geiss, Weak pitch angle scattering of few MV rigidity ions from measurements of anisotropies in the distribution function of interstellar pickup H^+, *Geophys. Res. Lett.*, *22*, 2665–2668, 1995.

Grappin, R., U. Frisch, J. Léorat, and A. Pouquet, Alfvénic fluctuations as asymptotic states of MHD turbulence, *Astron. Astrophys.*, *105* (1), 6–14, 1982.

Gray, P. C., C. W. Smith, W. H. Matthaeus, and N. F. Otani, Heating of the Solar Wind by Pickup Ion Driven Alfvèn Ion Cyclotron Instability, *Geophys. Res. Lett.*, *23*, 113–116, 1996.

Hollweg, J. V., Alfvén waves in the solar wind: Wave pressure, Poynting flux, and angular momentum, *J. Geophys. Res.*, *78*, 3643–3652, 1973.

Hollweg, J. V., Transverse Alfven waves in the solar wind: Arbitrary $\mathbf{k}$, $\mathbf{V}_0$, $\mathbf{B}_0$, and $|\delta\mathbf{B}|$, *J. Geophys. Res.*, *79*, 1539–1541, 1974.

Hollweg, J. V., On WKB expansions for Alfvén waves in the solar wind, *J. Geophys. Res.*, *95*, 14,873–14,879, 1990.

Hossain, M. and P. C. Gray, D. H. Pontius Jr., W. H. Matthaeus, and S. Oughton, Phenomenology for the Decay of Energy-Containing Eddies in Homogeneous MHD Turbulence, *Phys. Fluids*, *7*, 2886–2904, 1995.

Isenberg, P. A., A hemispherical model of anisotropic interstellar pickup ions, *J. Geophys. Res.*, *102*, 4719–4724, 1997.

Isenberg, P. A., and M. A. Lee, A dispersive analysis of bispherical pickup ion distributions, *J. Geophys. Res.*, *101*, 11,055–11,066, 1996.

Intriligator, D. S., G. L. Siscoe, and W. D. Miller, Interstellar pickup H^+ ipons at 8.3 AU: Pioneer 10 plasma and magnetic field analyses, *Geophys. Res. Lett.*, *23*, 2181–2184, 1996.

Johnstone, A. D., D. E. Huddleston, and A. J. Coates, The spectrum and energy density of solar wind turbulence of cometary origin, in *Cometary Plasma Processes*, Geophys. Monogr. Ser., vol. 61, edited by A. D. Johnstone, pp. 259–271, AGU, Washington, D.C., 1991.

King, J. H., and N. E. Papitashvili, Interplanetary Medium Data Book — Supplement 5, 1988–1993, (Rep. NSSDC/WDC–A–R&S 94–08, NASA, Greenbelt, Md) 1994.

Kinney, R., and J. C. McWilliams, Turbulent cascades in anisotropic magnetohydrodynamics, *Phys. Rev. E*, *57*, 7111–7121, 1998.

Kraichnan, R. H., and D. C. Montgomery, Two dimensional turbulence, *Rep. Prog. Phys.*, *43*, 547–619, 1980.

Leamon, R. J., C. W. Smith, N. F. Ness, W. H. Matthaeus and H. K. Wong, Observational constraints on the dynamics of the interplanetary magnetic field dissipation range, *J. Geophys. Res.*, *103*, 4775–4787, 1998a.

Leamon, R. J., W. H. Matthaeus, C. W. Smith, and H. K. Wong, Contribution of cyclotron-resonant damping to kinetic dissipation of interplanetary turbulence, *Astrophys. J. Lett.*, *507*, L181-L184, 1998b.

Leamon, R. J., C. W. Smith, N. F. Ness and H. K. Wong, Dissipation range dynamics: Kinetic Alfvén waves and the importance of β_e, *J. Geophys. Res.*, *104*, 22,331–22,344, 1999.

Leamon, R. J., W. H. Matthaeus, C. W. Smith, G. P. Zank, D. J. Mullan and S. Oughton, MHD driven kinetic dissipation in the solar wind and corona, *Astrophys. J.*, *537*, 1054–1062, 2000.

Lee, M. A., and W.-H. Ip, Hydromagnetic wave excitation by ionized interstellar hydrogen and helium in the solar wind, *J. Geophys. Res.*, *92*, 11,041–11,052, 1987.

Marsch, E., and C.-Y. Tu, Dynamics of correlation functions with Elsässer variables for inhomogeneous MHD turbulence, *J. Plasma Phys.*, *41*, 479–491, 1989.

Matthaeus, W. H. and S. Oughton, D. Pontius, and Y. Zhou, Evolution of energy containing turbulent eddies in the solar wind, *J. Geophys. Res.*, *99*, 19,267–19,287, 1994.

Matthaeus, W. H., J. W. Bieber, and G. P. Zank, Unquiet on any front: Anisotropic turbulence in the solar wind, *Rev. Geophys.*, U.S. Natl. Rep. Int. Union Geod. Geophys. 1991–1994, *33*, 609–614, 1995.

Matthaeus, W. H., G. P. Zank and S. Oughton, Phenomenology of hydromagnetic turbulence in a uniformly expanding medium, *J. Plasma Phys.*, *56*, 659–675, 1996.

Matthaeus, W. H., S. Oughton, S. Ghosh, and M. Hossain, Scaling of anisotropy in hydrodynamic turbulence, *Phys. Rev. Lett.*, *81*, 2056–2059, 1998.

Matthaeus, W. H., C. W. Smith and J. W. Bieber, Correlation Lengths, the Ultrascale, and the Spatial Structure of Interplanetary Turbulence, AIP Conf. Proc. 471: *Solar Wind 9*, edited by S. R. Habbal, R. Esser, J. V. Hollweg and P. A. Isenberg, American Institute of Physics, New York, 511–514, 1999.

Matthaeus, W. H., G. P. Zank, C. W. Smith and S. Oughton, Turbulence, Spatial Transport, and Heating of the Solar Wind, *Phys. Rev. Lett.*, *82*, 3444–3447, 1999.

McComas, D. J., B. L. Barraclough, H. O. Funsten, J. T. Gosling, E. Santiago-Muñoz, R. M. Skoug, B. E. Goldstein, M. Neugebauer, P. Riley, and A. Balogh, Solar wind observations over Ulysses' first full polar pass, *J. Geophys. Res.*, *105*, 10,419–10,433, 2000.

Möbius, E., M. A. Lee, P. A. Isenberg, D. Rucinski, and B. Klecker, *EOS Trans. AGU*, *76*(17), Spring Meeting Suppl. S229, 1995.

Montgomery, D. C., Major disruption, inverse cascades,

and the Strauss equations, *Phys. Scr., T, 2*(1), 83–88, 1982.

Murphy, N., E. J. Smith, B. T. Tsurutani, A. Balogh, and D. J. Southwood, Further studies of waves accompanying the solar wind pickup of interstellar hydrogen, *Space Sci. Rev., 72* (1–2), 447–453, 1995.

Murphy, N., E. J. Smith, J. Wolf, and D. S. Intriligator, A reexamination of "interstellar ion waves" previously identified in Pioneer 10 magnetic field data, *Geophys. Res. Lett., 25*, 3721–3724, 1998.

Oughton, S., E. R. Priest, and W. H. Matthaeus, The influence of a mean magnetic field on three-dimensional magnetohydrodynamic turbulence, *J. Fluid Mech., 280*, 95–117, 1994.

Oughton, S., S. Ghosh, and W. H. Matthaeus, Scaling of spectral anisotropy with magnetic field strength in decaying magnetohydrodynamic turbulence, *Phys. Plasmas, 5*, 4235–4242, 1998.

Richardson, J. D., K. I. Paularena, A. J. Lazarus, and J. W. Belcher, Radial evolution of the solar wind from IMP 8 to Voyager 2, *Geophys. Res. Lett., 22*, 325–328, 1995.

Richardson, J. D., J. L. Phillips, C. W. Smith and P. C. Gray, Thermal anisotropies in the solar wind: Evidence of heating by interstellar pickup ions?, *Geophys. Res. Lett., 23*, 3259–3262, 1996.

Roberts, D. A., M. L. Goldstein, and L. W. Klein, The amplitudes of interplanetary fluctuations: Stream structure, heliocentric distance, and frequency dependence, *J. Geophys. Res., 95*, 4203–4216, 1990.

Schwartz, S. J., W. C. Feldman, and S. P. Gary, The source of proton anisotropy in the high-speed solar wind, *J. Geophys. Res., 86*, 541–546, 1981.

Sharma, O. P., and V. L. Patel, Low-frequency electromagnetic waves driven by gyrotropic gyrating ion beams, *J. Geophys. Res., 91*, 1529–1534, 1986.

Shebalin, J. V., W. H. Matthaeus, and D. Montgomery, Anisotropy in MHD turbulence due to a mean magnetic field, *J. Plasma Phys., 29*, 525–547, 1983.

Smith, C. W., and J. W. Bieber, Multiple spacecraft survey of the north-south asymmetry of the interplanetary magnetic field, *J. Geophys. Res., 98*, 9401–9415, 1993.

Smith, E. J., et al., *EOS Trans. AGU, 75*(16), Spring Meeting Suppl. S297, 1994.

Sridhar, S., and P. Goldreich, Toward a theory of interstellar turbulence. I. Weak Alfvénic turbulence, *Astrophys. J., 432*, 612–621, 1994.

Taylor, G. I., Statistical theory of turbulence, *Proc. R. Soc. London, Ser. A, 151*, 421–444, 1935.

Tu, C.-Y., and E. Marsch, A model of solar wind fluctuations with two components: Alfvén waves and convective structures, *J. Geophys. Res., 98*, 1257–1276, 1993.

Tu, C.-Y., and E. Marsch, *MHD Structures, Waves and Turbulence in the Solar Wind*, Kluwer Acad., Norwell, Mass., 1995.

Tu, C.-Y., Z.-Y. Pu, and F.-S. Wei, The power spectrum of interplanetary Alfvénic fluctuations: Derivation of the governing equation and its solution, *J. Geophys. Res., 89*, 9695–9702, 1984.

Vasyliunus, V. M., and G. L. Siscoe, Flux and energy spectrum of interstellar ions in the solar system, *J. Geophys. Res., 81*, 1247–1252, 1976.

Verma, M. K., and D. A. Roberts, The radial evolution of the amplitudes of "dissipationless" turbulent solar wind fluctuations, *J. Geophys. Res., 98*, 5625–5630, 1993.

von Kármán, T., and L. Howarth, On the statistical theory of isotropic turbulence, *Proc. R. Soc. London Ser. A, 164*, 192–215, 1938.

Williams, L. L., and G. P. Zank, Effect of magnetic field geometry on the wave signature of the pickup of interstellar neutrals, *J. Geophys. Res., 99*, 19,229–19,244, 1994.

Williams, L. L., G. P. Zank, and W. H. Matthaeus, Dissipation of pickup-induced waves: A solar wind temperature increase in the outer heliosphere?, *J. Geophys. Res., 100*, 17,059–17,067, 1995.

Winske, D., and S. P. Gary, Electromagnetic instabilities driven by cool heavy ion beams, *J. Geophys. Res., 91*, 6825–6832, 1986.

Wu, C. S., and R. C. Davidson, Electromagnetic instabilities produced by neutral-particle ionization in interplanetary space, *J. Geophys. Res., 77*, 5399–5406, 1972.

Zank, G. P., Interaction of the solar wind with the local interstellar medium: A theoretical perspective, *Space Science Rev., 89*, 413–688, 1999.

Zank, G. P., and I. H. Cairns, Pickup ion driven turbulence in the polar heliosphere: A stochastic growth model, *Astrophys. J., 541*, 489–494, 2000.

Zank, G. P., and W. H. Matthaeus, Waves and turbulence in the solar wind, *J. Geophys. Res., 97*, 17,189–17,194, 1992a.

Zank, G. P., and W. H. Matthaeus, The equations of reduced magnetohydrodynamics, *J. Plasma Phys., 48*, 85–100, 1992b.

Zank, G. P., W. H. Matthaeus, and C. W. Smith, Evolution of turbulent magnetic fluctuation power with heliospheric distance, *J. Geophys. Res., 101*, 17,093–17,107, 1996.

Zank, G. P., J. A. Le Roux, W. H. Matthaeus, and H. Moraal, Solar wind turbulence, diffusion coefficients, and cosmic ray modulation, *Proc. 26^{th} Int. Cosmic Ray Conf., 7*, 41–44, 1999.

Zhou, Y., and W. H. Matthaeus, Transport and turbulence modeling of solar wind fluctuations, *J. Geophys. Res., 95*, 10,291–10,311, 1990.

C.W. Smith, W.H. Matthaeus, G.P. Zank, N.F. Ness Bartol Research Institute, University of Delaware, Newark, DE 19716. (e-mail: chuck@bartol.udel.edu, yswhm@bartol.udel.edu, zank@bartol.udel.edu and nfness@bartol.udel.edu

S. Oughton, Department of Mathematics, University College London, WC1E 6BT, England. (e-mail: sean@math.ucl.ac.uk)

J.D. Richardson, Building 37, Room 655, Massachusetts Institute of Technology, Cambridge, Massachusetts 02139. (e-mail: jdr@space.mit.edu)

This preprint was prepared with AGU's LaTeX macros v5.01. File lowlatheating formatted September 22, 2000.

With the extension package 'AGU++', version 1.2 from 1995/01/12